

## Amplitude-stabilized chaotic light

C. Radzewicz,\* Z. W. Li, and M. G. Raymer

*The Institute of Optics, University of Rochester, Rochester, New York 14627*

(Received 4 September 1987)

Large-bandwidth laser light pulses with pure frequency fluctuations have been generated. Chaotic-light pulses from a cavityless dye laser are temporally smoothed by passing them through strongly saturated amplifiers. Since the amplification process does not change the phase of the amplified light, the output radiation has the well-defined phase fluctuations of chaotic light, yet essentially no amplitude fluctuations.

### I. INTRODUCTION

All processes in nonlinear optics are sensitive to the nature of statistical fluctuations in laser light. Theoretical description and quantitative understanding of finite-bandwidth effects can be greatly simplified if the statistical properties of the fluctuating radiation field can be described by a simple model. So far, three such models have been used with considerable success. The phase-diffusion (PD) model assumes that the amplitude of the field is constant and its phase undergoes stochastic fluctuations, which can be described by the Brownian-motion diffusion equation. The output of an ideal single-mode cw laser operating far above threshold can be considered as phase-diffusion radiation.<sup>1</sup> However, in real lasers, other effects such as mechanical vibrations dominate and cause the light statistics to be far from that predicted by the PD model. The practical realization of radiation with properties close to those of the PD model was reported by Elliot *et al.*,<sup>2</sup> who used acousto- and electro-optic modulators outside the cavity of a well-stabilized single-mode dye laser to impose frequency and phase fluctuations on the laser light. By controlling the statistical properties of the electrical signal driving the modulators, they were able to produce radiation which could be described by the PD model up to the fourth-order correlation function of the field. Accurate measurements of two-photon absorption and optical double resonance were made with this system and good agreement was obtained with predictions of the PD model.<sup>2</sup> Many other optical processes have been treated theoretically using the PD model, including resonance fluorescence,<sup>3</sup> multiphoton absorption,<sup>4</sup> four-wave mixing,<sup>5</sup> and stimulated Raman scattering.<sup>6</sup>

Another model of laser light that has been used successfully to describe experiments is the multimode model, in which the field is taken to be composed of a sum of discrete frequency components, each with constant or slowly varying amplitude and random phase. For example, studies of stimulated Raman scattering that have been successfully described by the multimode model are reported in Ref. 7.

A third model that has proved to be useful is the chaotic-light (CL) model.<sup>1,8</sup> It assumes that the complex field amplitude undergoes fluctuations with statistics of a

random Gaussian process. Conventional thermal light sources like discharge lamps, etc., produce chaotic light. Also, it has been shown that for some applications a laser operating on many independent (uncoupled) modes can be considered, to some degree of approximation, as a chaotic-light source.<sup>9</sup> However, due to the finite number of discrete frequencies emitted by a multimode laser, the statistical properties of its radiation depart from that of the CL model, especially at low frequencies comparable with the mode spacing. It is also known that in high-gain lasers or amplifiers mode coupling effects lead to completely different radiation statistics.<sup>10-14</sup>

In this paper we describe a laser system that emits strong nanosecond light pulses with almost pure frequency fluctuations of well-defined statistics. A cavityless dye laser is used to produce broadband pulses of amplified spontaneous emission, which are believed to be well described by the chaotic-light model. These pulses are passed through saturated dye amplifiers, resulting in almost complete elimination of amplitude fluctuations.<sup>15</sup> Since the phase of the amplified light is preserved in the amplification process, the resulting radiation has the same phase fluctuations as chaotic light, yet essentially no amplitude fluctuations. To describe this new type of radiation, we use the phrase "amplitude-stabilized chaotic light."

The recent demonstration of the x-ray laser<sup>16</sup> has again raised previously studied questions concerning the temporal and spatial coherence properties of amplified spontaneous emission (ASE). The present study treats the highly saturated regime of ASE and makes new observations about the temporal behavior of the amplitude and phase of ASE under these conditions.

The paper is organized as follows. In Sec. II we describe the design and performance of a cavityless dye laser. Sections III and IV are devoted to the smoothing process and properties of amplitude-stabilized chaotic light. Section V summarizes the results.

### II. CAVITYLESS DYE LASER

It is known that spontaneous emission of a large number of molecules produces chaotic, or thermal, light.<sup>1</sup> This property is used to build a chaotic-light laser source. The design we applied has been used before (see, for ex-

ample, Ref. 17), although no systematic studies concerning the properties of the resulting radiation have been reported.

The laser is shown schematically in Fig. 1. It consists of a transversely pumped dye cell, telescope, and diffraction grating in Littrow arrangement. It lacks an output coupler of any kind; on the contrary, special care was taken to avoid any mechanisms leading to formation of cavity modes. Spontaneous emission from dye molecules is amplified on a single pass through the active medium, spectrally narrowed by the telescope and diffraction grating system and amplified further on the second pass through the dye cell. The output radiation of such a laser is expected to be chaotic as long as any mechanisms that lead to the coupling between different frequencies (equivalent to laser modes in a conventional laser) are avoided. In particular, gain saturation can lower the fluctuations in the output intensity and lead to nonchaotic statistics. Special care was taken to avoid etalon effects in the cavity which could produce undesirable structure in the laser spectrum. This was achieved by tilting the dye cell and placing the telescope far away (44 cm) from the dye cell. The distance from the dye cell to the diffracting grating (70 cm) was chosen such that the round-trip time was almost equal to the duration of the pump pulse (6 nsec). This prevents formation of cavity modes as a result of spurious backscatter from the dye-cell wall. Rhodamine 6G dye in methanol ( $6 \times 10^{-4}$  mol/liter) was used as an active medium. The pump pulses ( $\sim 1$  mJ) were provided by a frequency-doubled, *Q*-switched Nd:YAG laser (where YAG is yttrium aluminum garnet) operating in a single longitudinal mode and thus producing temporally smooth pulses. The cavityless dye-laser linewidth was about 7 GHz and the output energy was about  $10 \mu\text{J}$ .

Single-shot spectra of the dye-laser pulses were recorded with a Fizeau interferometer and photodiode array,<sup>10</sup> and an example of the results is shown in Fig. 2(a). No periodic structure could be noticed in the single-shot spectra; instead they displayed a continuous, random structure within the line envelope. Similar spectra were previously observed for a broadband color-center laser,<sup>18</sup> although their interpretation was somewhat different due to the presence of unresolved cavity-mode structure.

The interpretation of the observed spectra is based on the assumption that the laser emits chaotic light, whose complex field can be written in the form

$$\mathcal{E}(t) = p(t)E(t)e^{-i\omega_0 t}, \quad (2.1)$$

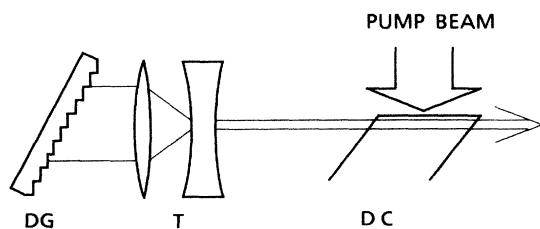


FIG. 1. Schematic diagram of cavityless dye laser: G, 3000 lines/mm holographic diffraction grating; T,  $12\times$  telescope; DC, dye cell.

where  $E(t)$  is a complex Gaussian random process,<sup>8</sup>  $p(t)$  is a smooth pulse envelope, and  $\omega_0$  is the center frequency. The field spectrum

$$\mathcal{E}(\nu) = \int \mathcal{E}(t)e^{-i2\pi\nu t} dt \quad (2.2)$$

is also a complex Gaussian process. Observed in the experiment was the frequency distribution of energy for a single shot, which is given by

$$S(\nu) = |\mathcal{E}(\nu)|^2, \quad (2.3)$$

and which displays large random fluctuations with characteristic frequency scale equal to  $1/T$ , where  $T$  is the pulse duration. The ensemble averaged spectrum  $\langle S(\nu) \rangle$  of the laser light is shown in Fig. 2(b). The average spectrum does not show any periodic structure, tentatively indicating the lack of any cavity modes. However, it is important to realize that such a structure can be washed out in this type of measurement by small frequency jitter in either the dye laser or Fabry-Perot interferom-

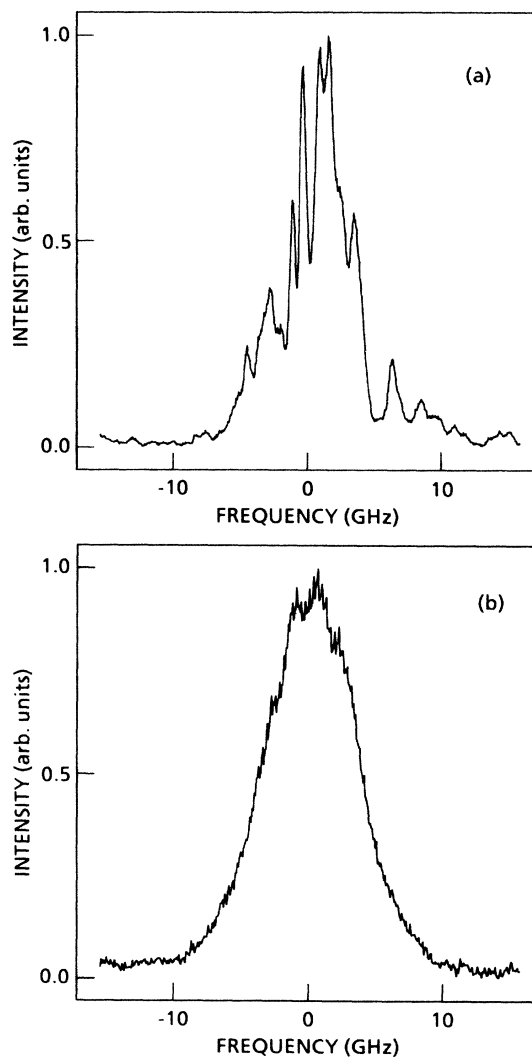


FIG. 2. (a) Single-shot spectrum of the cavityless dye laser light. (b) Average spectrum of 400 pulses from the cavityless dye laser. Zero on the frequency scale corresponds to the center frequency  $\omega_0$  of the light.

eter. Therefore, additional measurements were performed to better reveal the existence of any such mode structure. Using a Fizeau interferometer and photodiode array coupled to a computer we have measured many single-shot spectra, and from them calculated the spectrum autocorrelation function  $P(\nu)$ , defined as follows:

$$P(\nu) = \left\langle \int S(\nu') S(\nu' + \nu) d\nu' \right\rangle, \quad (2.4)$$

where  $\langle \rangle$  indicates an average over many laser pulses. Since  $P(\nu)$  depends only on the frequency difference and not on the absolute frequency, it is completely insensitive to the frequency jitter. It should be emphasized that  $P(\nu)$  depends both on amplitude and phase fluctuations of  $E(t)$ . This is contrary to the intensity autocorrelation function  $\langle |E(t)|^2 |E(t+\tau)|^2 \rangle$ , which depends only on

amplitude fluctuations. Since the knowledge of amplitude and phase behavior is necessary for a full description of the field, both intensity and spectrum correlation functions should be measured to provide such a description.  $P(\nu)$  measured for a cavityless dye laser is shown in Fig. 3. Weak features indicated by arrows in Fig. 3 are due to residual scattering from the dye-cell walls, which leads to slight enhancement in the correlation function for frequencies separated by  $c/2L$ , where  $L$  is the optical length of the dye cell. The central peak is directly connected to the stochastic nature of the radiation.

The spectrum autocorrelation function  $P(\nu)$  can be calculated for chaotic light. The frequency correlation function  $\langle S(\nu') S(\nu' + \nu) \rangle$  for CL was calculated by Masalov<sup>13</sup> using the moment theorem for Gaussian random variables,

$$\langle S(\nu') S(\nu' + \nu) \rangle = \langle S(\nu') \rangle \langle S(\nu' + \nu) \rangle \left[ 1 + \frac{\left| \int p(t) e^{-i2\pi\nu t} dt \right|^2}{\left| \int p(t) dt \right|^2} \right], \quad (2.5)$$

where  $p(t)$ , the smooth pulse envelope, is assumed to be the same for each pulse. Assuming

$$p(t) = \frac{T}{\sqrt{\pi}} \exp \left[ -\pi \left( \frac{t}{T} \right)^2 \right], \quad (2.6)$$

one obtains

$$\langle S(\nu') S(\nu' + \nu) \rangle = \langle S(\nu') \rangle \langle S(\nu' + \nu) \rangle \left\{ 1 + \exp \left[ -\left( \frac{\nu}{\Gamma} \right)^2 \right] \right\}, \quad (2.7)$$

where  $\Gamma = 1/(T\sqrt{2\pi})$ . In our case  $\Gamma$  is much smaller than the bandwidth of the laser and thus the factor  $\langle S(\nu') \rangle \langle S(\nu' + \nu) \rangle$  can be regarded as nearly constant in the range where the exponential factor in (2.7) is not vanishing. Thus the frequency correlation function is peaked around  $\nu=0$ , with the ratio of its peak value to the plateau value equal to 2.  $P(\nu)$  is analogous to the intensity autocorrelation function in the time domain and has basically the same form.

When the experimental data are considered, the finite resolution of the device measuring the spectrum has to be accounted for. This is done by introducing the instrumental function  $h(\nu - \nu_0)$ , which describes the spectral intensity measured by the interferometer when the incident radiation is monochromatic with frequency  $\nu_0$ . Then Eq. (2.4) is replaced by

$$P(\nu) = \left\langle \int d\nu' \int dx \int dy S(\nu') h(\nu' - x) S(\nu' + \nu) h(\nu' + \nu - y) \right\rangle. \quad (2.8)$$

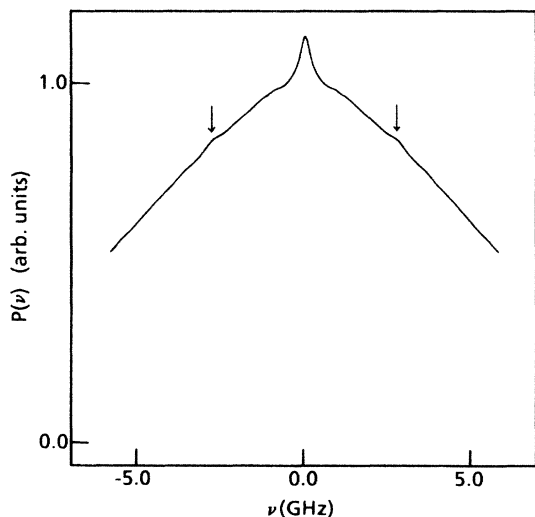


FIG. 3. Spectrum autocorrelation function for a cavityless dye laser.

A general analytic expression for the instrumental function of a Fizeau interferometer is not known<sup>19</sup> and thus an approximate expression will be used. We choose a Gaussian profile

$$h(\nu - \nu_0) = \frac{\gamma}{\sqrt{\pi}} \exp \left[ -\left( \frac{\nu - \nu_0}{\gamma} \right)^2 \right], \quad (2.9)$$

which makes the calculations easy to carry out. Here  $\gamma$  is the spectral resolution of the interferometer. Substituting Eq. (2.9) into Eq. (2.8) and using Eq. (2.7) gives

$$P(\nu) = \left[ 1 + \frac{\Gamma}{(2\gamma^2 + \Gamma^2)^{1/2}} \exp \left[ -\frac{\nu^2}{2\gamma^2 + \Gamma^2} \right] \right] \times \int \langle S(\nu') \rangle \langle S(\nu' + \nu) \rangle d\nu'. \quad (2.10)$$

If the averaged spectrum is wide compared to  $(2\gamma^2 + \Gamma^2)^{1/2}$ , then the expression  $\langle S(\nu') \rangle \langle S(\nu' + \nu) \rangle$  is approximately constant in the range of  $\nu$  where the ex-

ponential factor is not vanishing, and thus

$$P(\nu) \simeq \left[ 1 + \frac{\Gamma}{(2\gamma^2 + \Gamma^2)^{1/2}} \exp \left[ -\frac{\nu^2}{2\gamma^2 + \Gamma^2} \right] \right] \times \int \langle S(\nu') \rangle^2 d\nu' . \quad (2.11)$$

As can be seen from Eq. (2.11), the shape of  $P(\nu)$  strongly depends on the ratio  $\gamma/\Gamma$ . For  $\gamma \ll \Gamma$ , which corresponds to the spectral resolution much better than  $1/T$  the value  $P(0)$  is twice as large as  $P(\nu)$  in the plateau region. For  $\gamma$  comparable to  $\Gamma$ , the peak-to-plateau ratio is  $[1 + \Gamma/(2\gamma^2 + \Gamma^2)^{1/2}]$ . For  $\gamma \gg \Gamma$ ,  $P(\nu)$  is a flat function with no peak at  $\nu=0$ . The curve shown in Fig. 3 was measured with  $\Gamma=44$  MHz and  $\gamma=281$  MHz, so according to Eq. (2.11) the ratio of the peak to "plateau" (normalized to unity in the figure) should be equal to 1.11. The experimental value of this ratio as measured from Fig. 3 is equal to  $1.11 \pm 0.02$  and agrees well with the theoretical one. The error in this measurement is due to the fact that the wings of the experimental curve are falling, which is caused by the finite bandwidth of the laser. The theoretical value of this ratio is also an approximate one, due to the approximation used in Eq. (2.9).

In addition to spectral measurements, the intensity autocorrelation function  $\int \langle I(t)I(t+\tau) \rangle dt$ , where  $I(t) = |E(t)|^2$ , was measured using the standard frequency-doubling technique.<sup>20</sup> The result is shown in Fig. 4 (curve 1). The peak-to-plateau ratio is equal to 2 for stationary chaotic light.<sup>1</sup> We have measured the value  $1.9 \pm 0.1$  for this ratio.

In conclusion, the results of spectral and intensity autocorrelation measurements for a cavityless dye laser are in good agreement with the theoretical predictions for chaotic light. Although full characterization of statistical properties of given light requires measuring infinite

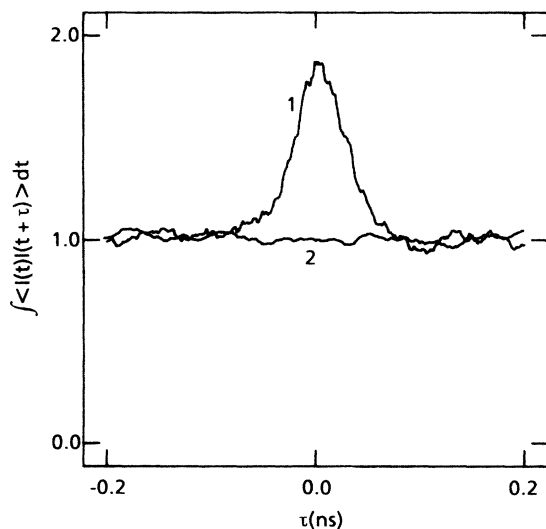


FIG. 4. Intensity autocorrelation functions of light from the cavityless dye laser before (curve 1) and after (curve 2) passing through the smoothing amplifier.

number of moments, we conclude that up through fourth order in the field the radiation of the cavityless dye laser can be modeled with good accuracy by the chaotic light model. It should be pointed out that unlike the laser with longitudinal modes, the cavityless laser produces light with a continuous spectrum and thus is a better approximation of a CL source.

It should also be mentioned that we were unable to obtain good results using the design for a cavityless dye laser given in Ref. 21. This is because with a short distance between dye cell and grating, light spuriously scatters from various surfaces, leading to multiple round trips and the formation of mode structure. This structure was not evident in the average spectrum  $\langle S(\nu) \rangle$  but was clearly evident in the spectral autocorrelation  $P(\nu)$ .

### III. PULSE-SMOOTHING AMPLIFIER

The principle of pulse smoothing has been described in a recent paper.<sup>15</sup> The method discussed in this reference is based on passing broadband, and thus intensity-fluctuating laser pulses through a saturated amplifier to which a nonsaturable absorber has been added and which is pumped by smooth laser pulses. It has been shown both theoretically and experimentally that such an amplifier produces smooth pulses that follow the pump pulse shape, regardless of intensity fluctuations in the input pulse. As an amplifying-absorbing medium, a solution of malachite green and rhodamine 6G dyes in methanol was used. We have observed that this solution is not chemically stable and deteriorates in time, which manifested itself as a decrease of the absorption at the laser wavelength. On the other hand, it was also demonstrated experimentally that significant but less effective smoothing can be achieved when no nonsaturable absorber was added. In the present paper we describe a design of a smoothing amplifier that avoids the chemical stability problems yet provides good smoothing of intensity fluctuations. It consists of two high-gain saturated amplifiers in series, with no nonsaturable absorber added. First a simple theoretical model will be presented, followed by the experimental data.

#### A. Theoretical analysis

A single-stage dye amplifier can be described in terms of rate equations,<sup>15</sup>

$$\frac{\partial I(t,z)}{\partial z} = [\sigma N_2(t,z) - \alpha] I(t,z) , \quad (3.1)$$

$$\frac{\partial N_2(t,z)}{\partial t} = \sigma_p I_p(t,z) N - [\sigma_p I_p(t,z) + \sigma I(t,z) + A] N_2(t,z) , \quad (3.2)$$

where  $I(t,z)$  is the photon flux of light being amplified,  $N_2(t,z)$  is the population of the upper level of laser transition,  $\sigma_p I_p(t,z)$  is the pump rate,  $A$  is the spontaneous decay rate of upper level,  $N$  is the concentration of dye molecules, and  $\sigma$  is the stimulated emission cross section.

Equations (3.1) and (3.2) have been written in a coordi-

nate system that moves with the amplified light pulse. The position  $z$  and time  $t$  are related to the laboratory position and time coordinates by  $z = z_{\text{lab}}$ ,  $t = t_{\text{lab}} - z_{\text{lab}}/v$ , where  $v$  is the velocity of light in the amplifying medium.

The coefficient  $\alpha$  describes the residual nonsaturable loss in the amplifier due to excited singlet absorption of the dye molecule<sup>22</sup> and diffraction of the beam traveling through a pumped region of small transverse dimensions ( $\sim 100 \times 100 \mu\text{m}$ ) in a long (2 cm) dye cell. However, estimation shows that a realistic value of  $\alpha$  is of the order of  $1 \text{ cm}^{-1}$ , thus the assumption  $\alpha L \gg 1$  ( $L$  is the amplifier cell length) is not valid and the analysis presented in Ref. 15 cannot be applied.

We assume that dispersion can be neglected in the relatively narrow range of frequencies covered by the laser line. We estimated that the maximum phase difference for different frequencies in a 10-GHz bandwidth due to dispersion of the active medium is smaller than  $2\pi/10$  in the case of our dye laser amplifier, which justifies the assumption of dispersionless medium. We also estimated self-phase modulation effects and found them to be small.

Effects of amplified spontaneous emission from the amplifier are neglected, thus Eqs. (3.1) and (3.2) do not apply to an amplifier in which the intensity of ASE is comparable to the intensity of amplified light. We assume that the pump pulses are provided by a single-mode laser and are temporally smooth. We also assume that the pump rate  $\sigma_p I_p(t, z)$  is much larger than the bandwidth of the input pulse, which means that the upper-level relaxation rate is much larger than the rate of temporal change of  $I(t, z)$ . This is an adiabatic approximation in which the amplifying medium at each point in space responds immediately to the changes of  $I(t, z)$  as well as  $I_p(t, z)$ , which is much slower. This point is discussed in more detail in Ref. 15. With this assumption, Eq. (3.2) can be integrated to give approximately

$$N_2(t, z) \simeq \frac{N \sigma_p I_p(t, z)}{\sigma_p I_p(t, z) + \sigma I(t, z)}, \quad (3.3)$$

where a spontaneous emission term has been neglected since it is small compared to  $\sigma_p I_p(t, z) + \sigma I(t, z)$ . Equation (3.3) is then substituted into Eq. (3.1), yielding

$$\frac{\partial I(t, z)}{\partial z} = \left[ \frac{g}{1 + I(t, z)/I_{\text{sat}}(t, z)} - \alpha \right] I(t, z), \quad (3.4)$$

where  $g = \sigma N$  is the unsaturated gain coefficient and  $I_{\text{sat}}(t, z) = (\sigma_p / \sigma) I_p(t, z)$  is the saturation intensity. Note that since the molecular system has no memory,  $\partial I(t, z) / \partial z$  depends only on local, current values of  $I$  and  $I_p$ . For a transversely pumped amplifier with uniform pumping,  $I_p$  (and thus  $I_{\text{sat}}$ ) depends only on the laboratory time  $t_{\text{lab}}$  and not the moving time variable  $t = t_{\text{lab}} - z/v$ . But in our case the amplifier path length is short ( $\sim 2 \text{ cm}$ ) so that the transit time  $L/v$  ( $\sim 60 \text{ ps}$ ) is much shorter than the time over which the pump pulse changes (duration  $\sim 6 \text{ nsec}$ ). So to good approximation we can replace  $I_p(t_{\text{lab}})$  by  $I_p(t)$ . This leaves Eq. (3.4) in the form of an ordinal differential equation with the independent  $t$  variable acting simply as a parameter

$$\frac{dI(t, z)}{dz} = \left[ \frac{g}{1 + I(t, z)/I_{\text{sat}}(t)} - \alpha \right] I(t, z), \quad (3.5)$$

with initial condition  $I(t, 0) = I(t_{\text{lab}} - L/v, 0)$ . This is a quasi-steady-state approximation in which  $I(t, z)$  instantaneously adjusts to the current value of  $I_{\text{sat}}$ . A saturated amplifier described by an equation similar to Eq. (3.5) was studied in detail by Curry *et al.* under the assumption of a weak pump.<sup>23</sup> In this regime  $I_{\text{sat}}$  is time independent and determined by molecular constants. They have found good energy stabilization for transform-limited, nanosecond pulses. However, no changes in the pulse shape were reported.

Equation (3.5) has been integrated numerically for fixed-medium length  $L$  and different values of  $g$  and  $\alpha$ , considering  $I_{\text{sat}}$  as a parameter. An example of the results for output intensity  $I(t, L) \equiv I_{\text{out}}$  versus input intensity  $I(t, 0) \equiv I_{\text{in}}$  is shown in Fig. 5(a) on a log-log scale. We are interested in reduction of relative intensity fluctuations; therefore, the quantity of interest is the "stabilization factor," defined as<sup>23</sup>

$$S = \frac{dI_{\text{in}}/I_{\text{in}}}{dI_{\text{out}}/I_{\text{out}}} = \frac{d \log_{10}(I_{\text{in}})}{d \log_{10}(I_{\text{out}})}, \quad (3.6)$$

which is the inverse of the slope of the curves in Fig. 5(a). As could be expected for very low and very high input intensities (unsaturated and totally bleached amplifier),  $S = 1$ . However, in the region of input intensities comparable to the saturation intensity,  $S$  is larger than 1, which means that relative intensity fluctuations are decreased by the amplifier. The smoothing properties of the amplifier depend strongly on the values of  $gL$  and  $\alpha L$ . The higher the value of  $gL$  the higher is the value of  $S$  calculated at  $I_{\text{in}} = I_{\text{sat}}$  and the larger is the range of input intensities over which  $S$  is large. However, in practice the  $gL$  product has to be limited in order to avoid saturation of the amplifier by its own amplified spontaneous emission, which is not included in our model. Note that in our analysis, the value of  $I_{\text{sat}}$  depends on the pump rate and is much higher than in a weakly pumped amplifier where  $I_{\text{sat}}$  is determined solely by the molecular constants. As can be seen in Fig. 5(a), considerable improvement in the performance of the smoothing amplifier can be achieved by increasing the loss coefficient  $\alpha$ , which was predicted by Curry *et al.*<sup>23</sup> and is also consistent with our previous result.<sup>15</sup> This can be explained as follows: In an amplifier with little or no loss and high gain, the intensity of amplified light increases rapidly as it travels through the amplifier and exceeds the range of intensities where the smoothing factor  $S > 1$ . However, if the loss experienced by the amplified beam is comparable to the unsaturated gain, the overall gain is positive for low intensities and negative for high intensities, which automatically leads to the reduction of fluctuations. In particular it has been shown<sup>23</sup> that for  $\alpha = \frac{1}{2}g$ , gain is positive for  $I < I_{\text{sat}}$  and negative for  $I > I_{\text{sat}}$  and the intensity stabilizes at  $I = I_{\text{sat}}$ , where the smoothing effect is the strongest. On the other hand, if losses are small, then dividing the amplifier into several stages can give good smoothing, provided that the beam is attenuated after each stage so its intensity does

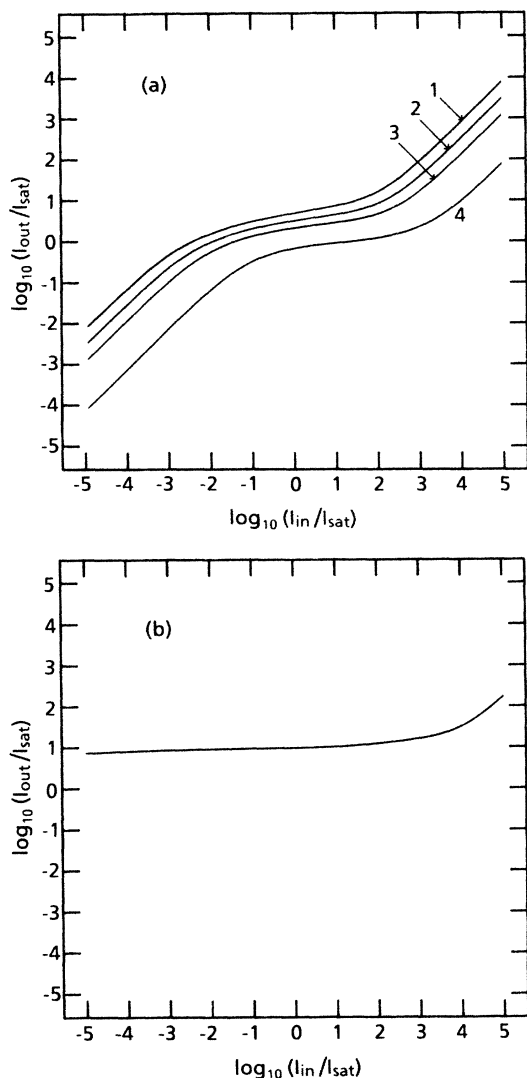


FIG. 5. Calculated output-vs-input characteristics for a saturated dye amplifier: (a) Single-stage amplifier with  $gL = 9.2$ ; curves 1, 2, 3, and 4 correspond to  $\alpha = 0$ ,  $\alpha = 0.1g$ ,  $\alpha = 0.2g$ , and  $\alpha = 0.5g$ , respectively. (b) Two-stage amplifier with each stage having  $gL = 9.2$  and  $\alpha = 0$ , with attenuation between stages equal to 500.

not exceed the saturation intensity. Input-output characteristics of a two-stage amplifier with  $\alpha = 0$  and  $gL = 9.2$  in each stage and 500 times attenuation between stages is shown in Fig. 5(b). This figure corresponds roughly to the configuration used in the experiments reported here. Notice that the range of input intensities over which output intensity remains nearly constant is much larger than that for a single-stage amplifier. This is desirable, especially if the input light is chaotic with full-scale intensity fluctuations.

An interesting question to be addressed is the following: What are the statistics of the output light from a smoothing amplifier if the input light is chaotic? If the probability distribution  $P(I_{in})$  for intensity of the input light is known, the corresponding distribution for the output radiation can be calculated by a simple mapping

of the input distribution into the output one with the help of the solutions of Eq. (3.5) and the relation

$$P(I_{out}) = \left| \frac{dI_{in}}{dI_{out}} \right| P(I_{in}). \quad (3.7)$$

Figure 6 shows an example of such a calculation. The input light was assumed to be chaotic with negative exponential distribution of intensity

$$P(I_{in}) = \langle I_{in} \rangle^{-1} \exp(-I_{in}/\langle I_{in} \rangle), \quad (3.8)$$

where  $\langle I_{in} \rangle$  is the average intensity and the two-stage amplifier transfer function is as shown in Fig. 5(b). It is clearly visible that the intensity fluctuations in the output light are much smaller and the resulting light pulses are smooth to within  $\pm 5\%$ .

### B. Experimental study of pulse smoothing

The predictions of the theoretical model were verified by experiment. Pulses from a cavityless dye laser were spectrally and spatially cleaned up with a diffraction grating and a pinhole and then amplified in a two-stage dye amplifier, which consisted of two transversely pumped dye cells filled with  $2.4 \times 10^{-4}$  mol/liter methanol solution of rhodamine 6G. The pump pulses for the amplifier (10 and 25 mJ for the first and second stage, respectively) were provided by the same single-mode, frequency-doubled Nd:YAG laser that was used to pump the cavityless dye laser. The pump rate was estimated to be larger than  $10^{11} \text{ s}^{-1}$ , which combined with a linewidth of the amplified light smaller than  $10^{10} \text{ s}^{-1}$  justifies the adiabatic approximation used in the theoretical description of the amplifier. Pump pulses for the amplifier were delayed to achieve good temporal overlap with the amplified pulse. The diverging output beam for the first amplifier stage propagated the distance 80 cm before entering the second amplifier stage. This provided the attenuation necessary

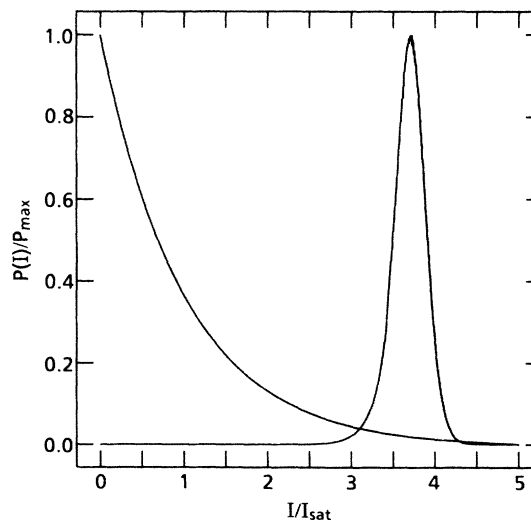


FIG. 6. Calculated intensity probability distribution for chaotic light (curve peaked at zero) and corresponding distribution (curve peaked at 3.7) after the two-stage amplifier with conditions the same as in Fig. 5(b).

to decrease the light intensity below saturation intensity at the input of the second amplifier. It also provided spatial filtering of the amplified beam. Because of the poor spatial quality of the pump beam the precise value of saturation intensity  $I_{\text{sat}} = (\sigma_p / \sigma) I_p$  cannot be calculated; coarse estimation showed it to be approximately  $10^8$  W/cm<sup>2</sup>. Also, the loss coefficient  $\alpha$  is rather difficult to calculate. Therefore the curves presented in Figs. 5 and 6 should be treated as an illustration rather than precise characteristics of the actual smoothing amplifier used in the experiment. The output energy of the two-stage amplifier was about 5 mJ.

The intensity fluctuations of the input and output pulses were recorded in two ways. For convenience a streak camera was used to observe time-resolved intensity during the alignment of the system. The time resolution of the streak camera (30 ps) was good enough to record all the intensity fluctuations of the 10-GHz-bandwidth radiation. An example of recorded traces is shown in Figs. 7(a) and 7(b) for the input and output pulses, respectively. The reduction of intensity fluctuations is clear. In the input pulse the fluctuations are comparable to the average intensity as should be expected for chaotic light, while in the output pulse the intensity fluctuations are much smaller than the average intensity. The residual fluctuations on the output trace are partially caused by noise in the streak camera.

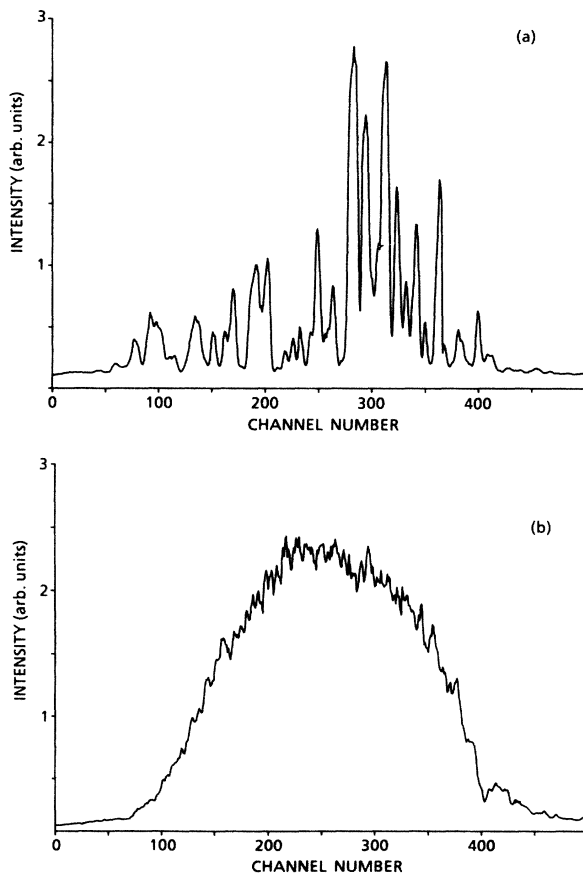


FIG. 7. Streak camera traces of laser pulses, 15 ps/channel: (a) cavityless dye laser output, (b) smoothing amplifier output.

In addition, the intensity autocorrelation function  $\int \langle I_{\text{out}}(t) I_{\text{out}}(t + \tau) \rangle dt$  of the output radiation was measured using the same technique as described in Sec. II and the result is shown in Fig. 4 (curve 2). Intensity fluctuations would show up as a peak at  $\tau=0$ . Taking into account noise present in the measurement, we can say that no peak higher than 5% of the plateau value exists. The results of both streak camera and intensity autocorrelation measurements show that a considerable reduction in intensity fluctuations can be achieved in the described amplifier, leading to an almost purely phase fluctuating field.

#### IV. EVOLUTION OF SPECTRUM AND PHASE OF SMOOTHED LIGHT

Additional measurements were performed to establish if the smoothing amplifier changes the phase of the amplified radiation. The experimental setup is shown in Fig. 8(a). A part of the input beam was combined with the attenuated output beam on a beam splitter BS2. In this way a Mach-Zehnder interferometer was formed which included the amplifier in one of its arms. We searched for a fringe pattern in the observation plane  $O$ . As should be expected, no fringes could be detected if the

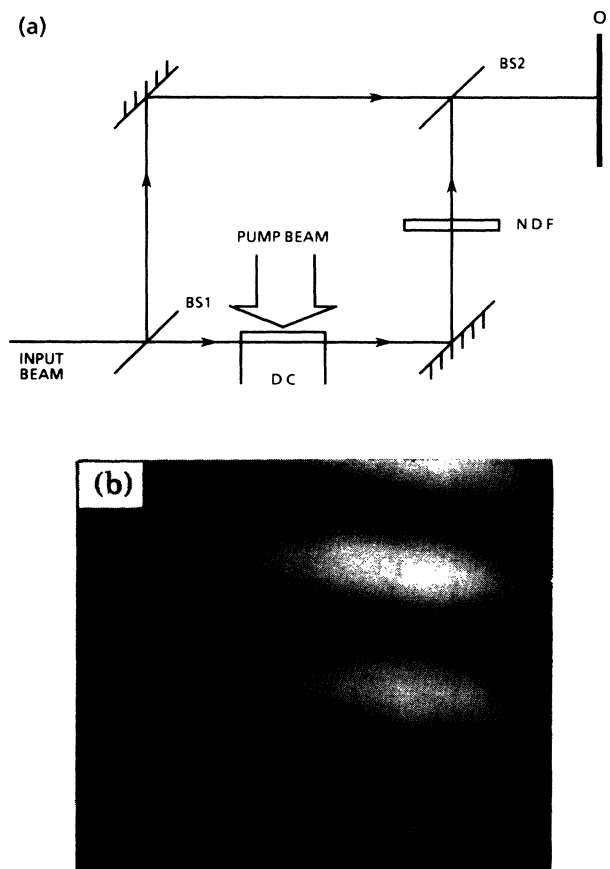


FIG. 8. (a) Experimental setup used to determine the change of phase in the smoothing amplifier. BS1, BS2, beam splitters; DC, dye cell; NDF, neutral density filter; O, observation plane. (b) Photograph of the fringe pattern from the Mach-Zehnder interferometer.

path difference in the two arms of the interferometer was larger than the coherence length of the laser light ( $\sim 5$  cm). However, if this path difference was chosen to be near zero, a clear fringe pattern was observed as shown in Fig. 8(b). Formation of such a fringe pattern is possible only if the phases of light in both beams are nearly the same. Therefore we conclude that the smoothing amplifiers did not significantly change the phase of the amplified light. This is consistent with the neglect of dispersion in our theoretical model described earlier.

This allows us to deduce the probability distribution of phase for the smoothed light. To do that, we assume, for simplicity, that the smoothing process is perfect, i.e., the output pulses have constant field amplitude except for a slowly varying envelope. We also assume that the phase of the amplified light does not change in the amplification process. This cannot be deduced from our rate-equation model, however, an experimental proof was presented above. The amplitude of input chaotic field [see Eq. (2.1)] can be written in the form

$$E(t) = E_R(t)e^{i\Psi(t)}, \quad (4.1)$$

where  $E_R(t)$  is a real valued fluctuating amplitude of chaotic light,  $\Psi(t)$  is its phase, and the slowly varying envelope  $p(t)$  was omitted. The output field is then given by

$$E_{\text{out}}(t) = E_R^0 e^{i\Psi(t)}, \quad (4.2)$$

with a constant real amplitude  $E_R^0$ . The output field is purely frequency fluctuating and its phase fluctuations are those of chaotic light. Elementary concepts of statistics<sup>1,8</sup> can be used to show that the probability distribution function  $P(\Psi)$  for the phase of chaotic light is uniform,

$$P(\Psi) = \frac{1}{2\pi}. \quad (4.3)$$

Since, as has been mentioned before, the amplifier does not change the phase of amplified light, the phase distribution for the output light from the amplifier is also given by Eq. (4.3).

The single-shot spectrum of the smoothed light was measured using the same method as that applied for measuring the spectrum of cavityless laser light. Random structure similar to that in Fig. 2(a) was observed. Thus, the intensity smoothing process does not also smooth the spectrum. In addition, the average spectrum of the smoothed light was measured. We found that the average spectra of chaotic light and smoothed light are the same within the accuracy of our measurement. We found this result somewhat surprising so a theoretical model was developed to explain it.

To model the spectrum of the smoothed light a numerical simulation was performed. A series of pulses of chaotic light with field  $E(t)$  was generated numerically by integrating the Langevin's equation

$$\frac{\partial E(t)}{\partial t} = -\gamma E(t) + F(t), \quad (4.4)$$

where  $\gamma^{-1}$  is the coherence time and  $F(t)$  is a complex,  $\delta$ -correlated, Gaussian random variable.  $E_{\text{out}}(t)$  was then calculated using Eq. (4.2), with  $\Psi(t)$  given by the phase of

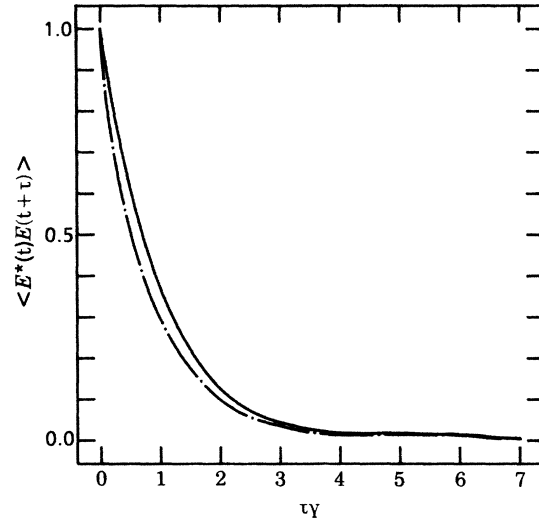


FIG. 9. Numerically simulated autocorrelation functions  $\langle E(t)E(t+\tau) \rangle$  (solid curve) and  $\langle E_{\text{out}}^*(t)E_{\text{out}}(t+\tau) \rangle$  (dashed-dotted curve) for chaotic light and amplitude-stabilized chaotic light, respectively.

the input chaotic light generated by integrating Eq. (4.4). Then the autocorrelation functions  $\langle E^*(t)E(t+\tau) \rangle$  and  $\langle E_{\text{out}}^*(t)E_{\text{out}}(t+\tau) \rangle$  were calculated, giving the results shown in Fig. 9. The autocorrelation function for the simulated chaotic field  $E(t)$  was found to be in good agreement with the theoretical negative-exponential formula  $\exp(-\gamma|\tau|)$ . As can be seen from Fig. 9, the autocorrelation function for the smoothed light decays faster than that for the chaotic light, but the curves are almost identical for times longer than  $\gamma^{-1}$ .

Average optical spectra for both input and output fields were calculated by computing the Fourier transform of corresponding autocorrelation functions and averaging over 20 realizations. The results are shown in Fig. 10. Except for noise caused by the rather small

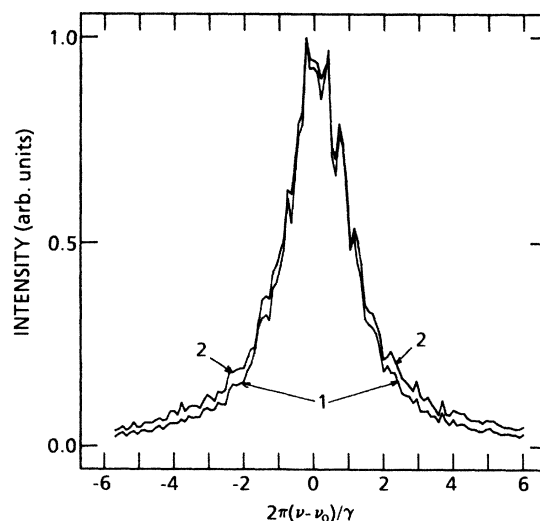


FIG. 10. Numerically simulated, average optical spectra of chaotic light (curve 1) and amplitude-stabilized light (curve 2);  $\nu_0$  is the center frequency of the laser line.



number of field realizations used in the calculations, the chaotic-light spectrum can be well fitted with a Lorentzian curve. As can be seen in Fig. 10, the two spectra are similar in the range of frequencies  $\nu$  close the center frequency  $\nu_0$  ( $|\nu - \nu_0| \lesssim \gamma/2\pi$ ). This is consistent with the fact that corresponding autocorrelation functions are almost the same for times longer than  $\gamma^{-1}$ . The only difference between the two spectra is in the wings of the two curves ( $|\nu - \nu_0| > \gamma/2\pi$ ), where the smoothed-light spectral intensity is slightly higher than that for chaotic light. This is due to the faster decay of the autocorrelation function for smoothed light in the range of times shorter than  $\gamma^{-1}$ .

The calculations are consistent with the results of measurements in the sense that no appreciable increase of the full width at half maximum occurred. Due to the noise in the experiment we were not able to observe the predicted increase of the wings in the spectrum of smoothed light.

### V. SUMMARY

A cavityless dye laser was carefully characterized via measurements of spectral and intensity autocorrelation

functions and was found to emit light described by the chaotic model, at least up to fourth order in the field. A two-stage saturated dye amplifier pumped by a single-mode Nd:YAG laser was used to reduce amplitude fluctuations of chaotic light from the cavityless dye laser. The intensity of the output pulses from the amplifier is smooth, while the phase is rapidly fluctuating. It was demonstrated that the dye amplifier does not change the phase of the light. Therefore the output field has the same stochastic phase fluctuations as chaotic light, which has a uniform phase distribution. The average spectrum of the amplitude-stabilized chaotic light is found to be nearly the same as that of chaotic light, at least within the central part of the line.

### ACKNOWLEDGMENTS

Several helpful discussions with Sven Hartmann and Rajarshi Roy are gratefully acknowledged. This research was supported in part by the U.S. Army Research Office.

\*Permanent address: Physics Department, Warsaw University, Warsaw, Poland.

<sup>1</sup>R. Loudon, *The Quantum Theory of Light* (Clarendon, Oxford, 1983).

<sup>2</sup>D. S. Elliott, R. Roy, and S. J. Smith, *Phys. Rev. A* **26**, 12 (1982); D. S. Elliot, M. W. Hamilton, K. Arnett, and S. J. Smith, *Phys. Rev. Lett.* **53**, 439 (1984).

<sup>3</sup>J. H. Eberly, *Phys. Rev. Lett.* **37**, 1387 (1976); G. S. Agarwal, *ibid.* **37**, 1383 (1976).

<sup>4</sup>L. Allen and C. R. Stroud, *Phys. Rep.* **91**, 3 (1982).

<sup>5</sup>G. S. Agarwal and S. Singh, *Phys. Rev. A* **25**, 3195 (1982).

<sup>6</sup>M. G. Raymer, J. Mostowski, and J. L. Carlsten, *Phys. Rev. A* **19**, 2304 (1979).

<sup>7</sup>W. R. Truntna, Jr., Y. K. Park, and R. L. Byer, *IEEE J. Quantum Electron.* **QE-15**, 648 (1979); J. Rifkin, M. L. Bernt, D. C. MacPherson, and J. L. Carlsten (unpublished).

<sup>8</sup>J. W. Goodman, *Statistical Optics* (Wiley, New York, 1985).

<sup>9</sup>J. L. DeBethune, *Nuovo Cimento B* **12**, 101 (1972); G. Mainfray, in *Multiphoton Processes*, edited by J. H. Eberly and P. Lambropoulos (Wiley, New York, 1977).

<sup>10</sup>L. A. Westling, M. G. Raymer, and J. J. Snyder *J. Opt. Soc. Am. B* **1**, 150 (1984).

<sup>11</sup>L. A. Westling and M. G. Raymer, *J. Opt. Soc. Am. B* **3**, 911 (1986).

<sup>12</sup>N. B. Abraham, J. C. Huang, D. A. Kranz, and E. B. Rockpower, *Phys. Rev. A* **24**, 2556 (1981).

<sup>13</sup>A. V. Masalov, in *Progress in Optics*, edited by E. Wolf (North-Holland, Amsterdam, 1985), Vol. 22, p. 145.

<sup>14</sup>F. A. Hopf, *Phys. Rev. Lett.* **56**, 2800 (1986).

<sup>15</sup>Z. W. Li, C. Radzewicz, and M. G. Raymer, *Opt. Lett.* **12**, 416 (1987).

<sup>16</sup>D. L. Mathews *et al.*, *Phys. Rev. Lett.* **54**, 110 (1985); S. Suckewer, C. H. Skinner, H. Milchberg, C. Keane, and D. Voorhees, *ibid.* **55**, 1753 (1985).

<sup>17</sup>R. Beach and S. R. Hartman, *Phys. Rev. Lett.* **53**, 663 (1984).

<sup>18</sup>V. M. Baev, G. Gaida, H. Schröder, and P. E. Toschek, *Opt. Commun.* **38**, 309 (1981).

<sup>19</sup>T. A. Hall, *J. Phys. E* **2**, 837 (1969).

<sup>20</sup>D. J. Bradley and G. H. C. New, *Proc. IEEE* **62**, 313 (1974).

<sup>21</sup>P. Ewart, *Opt. Commun.* **55**, 124 (1985).

<sup>22</sup>E. Sahar and D. Treves, *IEEE J. Quantum Electron.* **QE-13**, 962 (1977).

<sup>23</sup>S. M. Curry, R. Cubeddu, and T. H. Hänsch, *Appl. Phys.* **1**, 153 (1973).

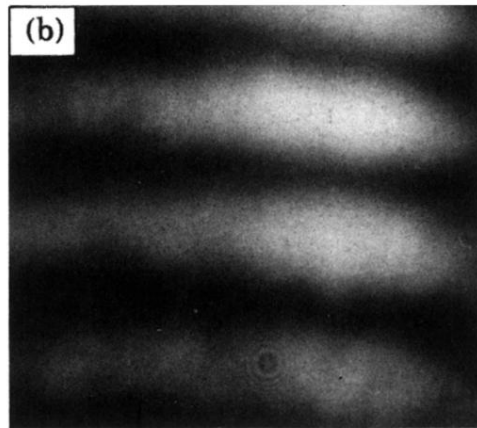
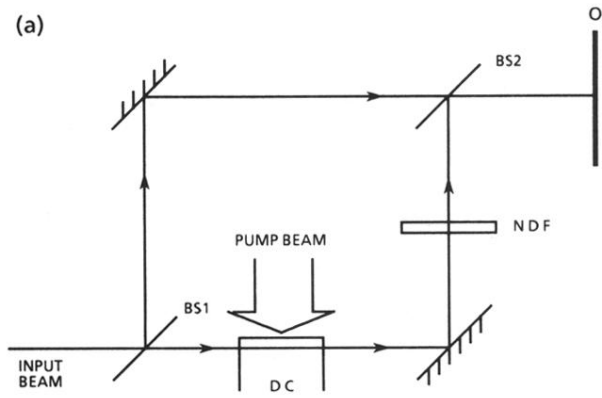


**FIG. 8.** (a) Experimental setup used to determine the change of phase in the smoothing amplifier. BS1,BS2, beam splitters; DC, dye cell; NDF, neutral density filter; *O*, observation plane. (b) Photograph of the fringe pattern from the Mach-Zehnder interferometer.